

# Using edge direction information for measuring blocking artifacts of images

F. Pan · X. Lin · S. Rahardja · E. P. Ong · W. S. Lin

Received: 6 December 2005 / Revised: 7 August 2006 /  
Accepted: 24 August 2006 / Published online: 24 February 2007  
© Springer Science+Business Media, LLC 2007

**Abstract** Block-based transform coding is the most popular approach for image and video compression. The objective measurement of blocking artifacts plays an important role in the design, optimization, and assessment of image and video coding systems. This paper presents a new algorithm for measuring blocking artifacts in images and videos. Instead of using the traditional pixel discontinuity along the block boundary, we use the edge directional information of the images. The new algorithm does not need the exact location of the block boundary thus is invariant to the displacement, rotation and scaling of the images. Experiments on various still images and videos show that the new blockiness measure is very efficient in terms of computational complexity and memory usage, and can produce blocking artifacts measurement consistent with subjective rating.

**Keywords** Image compression · Block-based transform coding · Perceptual metrics · Blocking artefacts · Un-referenced metrics

---

W. S. Lin  
School of Computer Engineering,  
Nanyang Technological University,  
Block N4, Nanyang Avenue, Singapore 639798  
e-mail: weisi@ieee.org

X. Lin · S. Rahardja · E. P. Ong  
Institute for Infocomm Research,  
21 Heng Mui Keng Terrace, Singapore, 119613

F. Pan (✉)  
ViXS Systems Inc., 245 Consumers Road, Toronto, ON M2J 1R3 Canada  
e-mail: edwardfpan@hotmail.com

## 1 Introduction

Block transform coding is the most popular approach for image and video coding. Most of the state of the art image and video coding standards, such as JPEG, H.26x and MPEG-1/2/4, make use of the block-based discrete cosine transform (BDCT) (Shi and Sun, 1999). In BDCT coding, DCT coefficients are calculated over small non-overlapping blocks, and the 2D blocks of transform coefficients are then quantized, zigzag scanned, and entropy coded. In the decoder, the quantized transform coefficients are de-quantized, and inverse transformed to recover the original data (with certain distortion). At low bit rate image and video coding, a large quantization step size is used. Therefore, the decompressed image and video exhibits various kinds of distorted artifacts. One of the most noticeable artifacts is the “blocking artifact,” which is an artificial discontinuity between adjacent blocks and is a direct result of the independent quantization of the transform coefficients (Karunasekera & Kingsbury, 1995; Miyahara, Kotani, Algazi, 1998; VQEG, 2000; Wang et al., 2002; Wu & Yuen, 1997). These blocking artifacts are structural disturbance, and are sometimes “buried” in the massively accumulated across-the-board pixel-wise error. Therefore their significance in perceptual visual quality assessment is not reflected correctly in the conventional peak signal-to-noise ratio (PSNR) measure. An effective measure of blocking artifacts is indispensable and can be used as a quality metric alone (Karunasekera & Kingsbury, 1995; Wang et al., 2002; Wu & Yuen, 1997) or one of many factors in quality evaluation (Miyahara, Kotani, Algazi, 1998; VQEG, 2000; Yu, Wu, Winkler, Chen, 2002).

There are generally two types of objective image and video quality metrics, i.e., referenced approach and un-referenced approach. In a referenced approach, the access to original images is required. By using the original and reproduced image as inputs, the system outputs a numerical value that quantifies the visibility of blocking artifacts in the reproduced image (Karunasekera & Kingsbury, 1995). This approach is not very useful in applications such as image and video communication, where original image and video is not accessible. On the other hand, the un-referenced approach (Wang et al., 2002; Wu & Yuen, 1997) is of more interests because of its computational efficiency and wider scopes of potential applications, including in-service visual quality monitoring and post-processing for decoded signal. However, designing un-referenced objective quality metrics is very difficult due to the limited understanding of the human vision system (HVS). It is believed that effective un-referenced objective quality metrics are only feasible when the prior knowledge about the image distortion types is available (Karunasekera & Kingsbury, 1995; VQEG, 2000; Wang et al., 2002; Wu & Yuen, 1997).

The generalized block-edge impairment metric  $M_{GBIM}$  proposed in Wu and Yuen (1997) evaluates the visual significance of block-edge artifacts in a given image by taking into account the luminance masking effects in extreme bright/dark areas in a reconstructed image. Wang et al. (2002) has proposed an un-referenced perceptual quality assessment of JPEG compressed images based on the measures of blockiness and image signal activity, and these two measures are then combined in a model whose parameters are estimated from the subject test data.

In this paper, a new algorithm is proposed to calculate the blocking artifacts in BDCT-coded image and video. Compared with the existing algorithms, this new method does not need the exact location of the block boundary thus is invariant to the displacement, rotation and scaling of the images. The method will also provide the information as to if and how the images have been altered. Experiments on various

still images and video frames show that the new measure can produce consistent blockiness measures for images of different types and subject to different amount of compression.

The rest of the paper is organized as follows: Section 2 presents the un-referenced approach for measuring blocking artifacts in BDCT coded images based on the edge directional information. Section 3 presents the experimental results, and its comparison with some of the existing schemes. Section 4 provides the conclusions of the paper.

## 2 Edge direction based blocking artifacts measurement

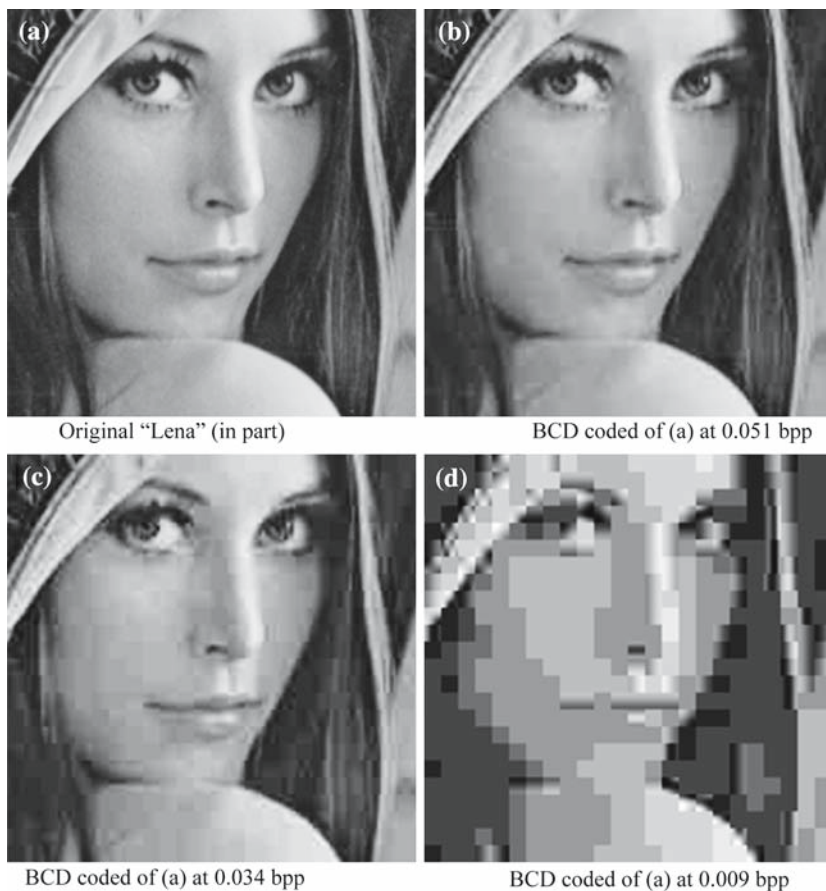
As mentioned in the Introduction, the blocking artifacts manifest itself as an artificial discontinuity between neighboring blocks. This is the direct result of the large quantization step size used in the encoding process, and the independent processing of these blocks that does not take into account the cross-block pixel correlations. A typical phenomenon of blocking artifacts is that the inter-pixel differences of cross-block pixels are much bigger than that of the in-block pixels. In this section, we will discuss another important impact of the BDCT coding on the images, i.e., the orientation changes of the edge pixels and their relationship with the blocking artifacts caused by the BDCT coding.

### 2.1 Edge direction histogram and blocking artifacts

As mentioned previously, when the blocking artifacts become severe, discontinuity between neighboring blocks becomes more obvious. This is only due to the change of the amplitude of the pixel. By examining the edge orientation of those pixels in the boundary of  $8 \times 8$  blocks as shown in Fig. 1, we can notice that the edge orientation of these pixels will change accordingly as the quantization values used in BDCT coding increases. Typically, as the quantization value increases, the blocking artifacts become more severe, and more and more edge pixels align in the orientation of  $0^\circ$  and  $90^\circ$ , or become inactive or “flat.” Figure 2 shows an example of such trend for image “Mandrill.” It is noted that the number of pixels that have the orientation of  $0^\circ$  and  $90^\circ$ , or “flat” increase monotonically as the quantization value increases, which is interpreted as the bits-per-pixel decreases in Fig. 2.

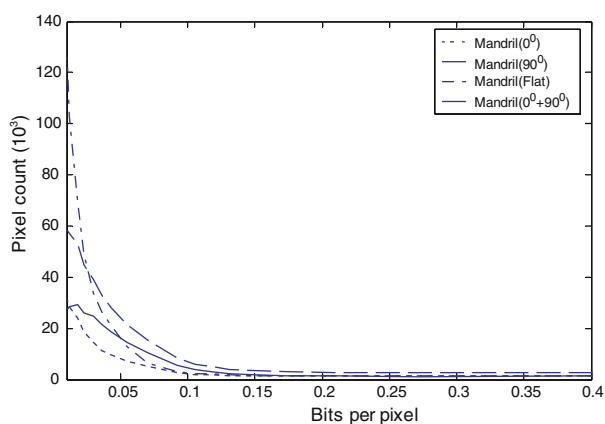
Figure 3 shows the pixel arrangement of an  $8 \times 8$  block. It is obvious that, as is manifested in Fig. 3, those pixels marked with “H” will tend to have edge orientation of  $0^\circ$ , those marked with “V” will tend to have edge orientation of  $90^\circ$ , and those marked with “D” will tend to have edge orientation in the diagonal direction. As to the pixels marked with “Z,” their edge intensity will become smaller and smaller due to the loss of high frequency details. Therefore, by examining the edge direction changes of these pixels we will be able to find how severe the blocking artifacts are.

Figures 4 and 5 shows the edge direction histograms of original image “Lena,” “Mandrill,” and their BDCT coded counterpart. From these figures we can see that these images and their BDCT coded counterparts have similar edge direction histograms in most of the other edge directions, except that the BDCT coded images have very strong edge direction presences at  $0^\circ$  and  $90^\circ$ , which is the result of the abrupt inter-pixel discontinuity of cross-block pixels in the horizontal direction and vertical direction. It is also noted that as the blocking artifacts become more severe,



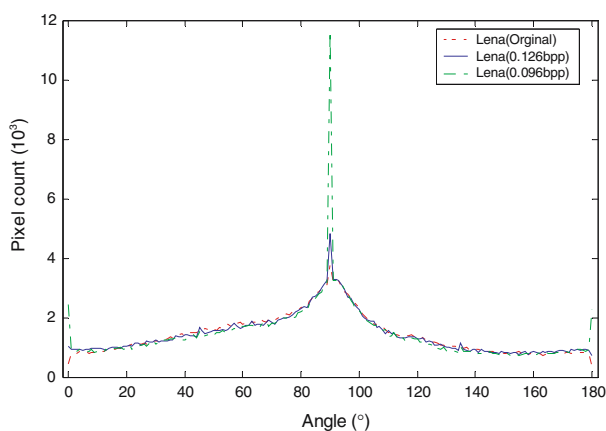
**Fig. 1** The pixels' edge orientation change as the quantization values used in BDCT coding increases. (a) Original "Lena" (in part) (b) BCD coded of (a) at 0.051 bpp (c) BCD coded of (a) at 0.034 bpp (d) BCD coded of (a) at 0.009 bpp

**Fig. 2** More and more pixels align in the edge orientation of  $0^\circ$ ,  $90^\circ$ , or become "flat"



**Fig. 3** Edge orientations of pixels in an  $8 \times 8$  block

D	H	H	H	H	H	H	D
V	Z	Z	Z	Z	Z	Z	V
V	Z	Z	Z	Z	Z	Z	V
V	Z	Z	Z	Z	Z	Z	V
V	Z	Z	Z	Z	Z	Z	V
V	Z	Z	Z	Z	Z	Z	V
V	Z	Z	Z	Z	Z	Z	V
D	H	H	H	H	H	H	D

**Fig. 4** Edge direction histograms of “Lena” and its BDCT coded image

more and more edge pixels will align in these two directions, and more pixels become inactive or “flat.” Therefore the proportion of the orientation of edges along these two directions as well as becoming “flat” in an image is a very good indication how severe the blocking artifacts are.

A very interesting and useful feature of the edge direction histogram is that, if the BDCT coded image is rotated at angle  $\alpha$ , there are still two strong edge direction presences around the angle  $(\alpha + 0^\circ)$  and  $(\alpha + 90^\circ)$ . Note that the amplitude of these two spikes has been reduced and their width has been increased. This indicates that there is similar amount of energy around these two angles. It is noted that the reduction in the amplitude and increase in the width is basically due to the discrete nature of the images. Figure 6 shows the edge direction histograms of “Lena” and its BDCT coded image after rotating  $10^\circ$ .

## 2.2 Construction of the edge direction histogram

The pixel gradient vectors in an image are determined by the gradient vector  $[G_x(x, y), G_y(x, y)]^T$ , which can be approximated by using the following Sobel operator (Gonzalez & Woods, 2002):

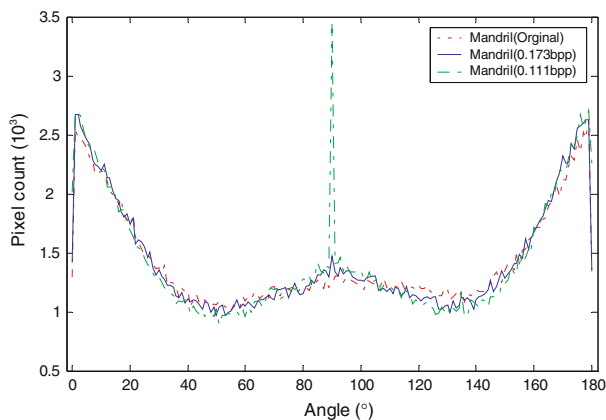


**Fig. 5** Edge direction histograms of “Mandrill” and its BDCT coded image

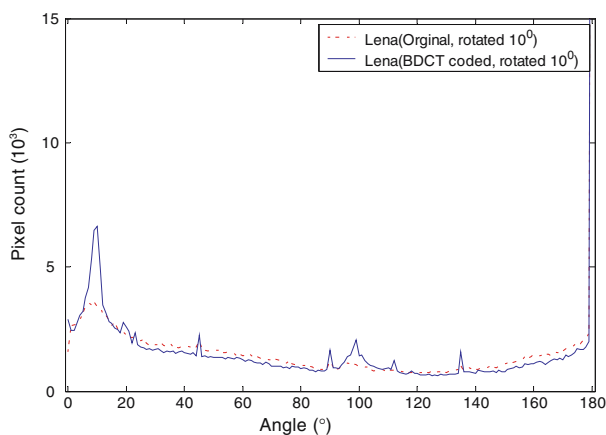


**Fig. 6** Edge direction histograms of “Lena” and its BDCT coded images after rotating 10°

$$\begin{aligned}
 G_x(x, y) &= -I(x-1, y-1) - 2 \times I(x-1, y) - I(x-1, y+1) \\
 &\quad + I(x+1, y-1) + 2 \times I(x+1, y) + I(x+1, y+1), \\
 G_y(x, y) &= I(x-1, y+1) + 2 \times I(x, y+1) + I(x+1, y+1) \\
 &\quad - I(x-1, y-1) - 2 \times I(x, y-1) - I(x+1, y-1),
 \end{aligned} \quad (1)$$

where  $I(x, y)$  represents the pixel intensity at location  $(x, y)$  in an image. In order to reduce the noise effect caused by the digitization of the images, the edge direction histogram is based on the local average of the pixel gradient vectors. The purpose of “averaging” the gradient vectors is to cancel vectors when they are perpendicular to each other, and to reinforce each other when they are pointing to the same direction or pointing to the opposite direction, as the opposite gradient vectors indicate the same edge orientation. A well established solution to this problem is to double the angles of the gradient vectors before averaging (Bazen & Gerez, 2002; Kass & Witkin, 1987). After doubling the angles, opposite gradient vectors will point to the same direction and reinforce each other, while perpendicular gradients will cancel each other. For

example, two perpendicular vectors with  $0^\circ$  and  $90^\circ$ , will have orientation of  $0^\circ$  and  $180^\circ$  after doubling their angles, and will cancel each other after averaging, and opposite vectors with  $0^\circ$  and  $180^\circ$ , will have orientation of  $0^\circ$  and  $360^\circ$  after doubling, and will reinforce each other when averaged.

Mathematically, doubling the angles is equivalent to squaring the complex number representation of the gradient vectors. Note that the length of the gradient vectors is squared, which has the effect that strong orientations have a higher votes in the average orientation than weaker orientations before averaging, which is equivalent to doubling the angles of the gradient vectors.

$$(G_x + jG_y)^2 = G_x^2 - G_y^2 + j2G_xG_y \quad (2)$$

and the average squared gradient can be calculated by averaging in local neighborhood, using a possible non-uniform window  $W$ ,

$$DF_x = \sum_W (G_x^2 - G_y^2), \quad DF_y = \sum_W (2G_xG_y). \quad (3)$$

Now, the averaged gradient direction  $\phi$ , with  $-90^\circ \leq \phi \leq 90^\circ$ , is defined as

$$\phi(x, y) = \frac{1}{2} \angle (DF_x, DF_y), \quad (4)$$

where  $\angle(x, y)$  is defined as,

$$\angle(x, y) = \begin{cases} \frac{180^\circ}{\pi} \tan^{-1} \left( \frac{y}{x} \right) & x \geq 0, \\ \frac{180^\circ}{\pi} \tan^{-1} \left( \frac{y}{x} \right) + 180^\circ & \text{for } x < 0 \wedge y \geq 0, \\ \frac{180^\circ}{\pi} \tan^{-1} \left( \frac{y}{x} \right) - 180^\circ & x < 0 \wedge y < 0 \end{cases} \quad (5)$$

and the edge direction,  $\theta(x, y)$ , which is perpendicular to the gradient direction, is defined as,

$$\theta(x, y) = \phi(x, y) + 90^\circ. \quad (6)$$

Note that the about angle,  $\theta(x, y)$ , has a range from  $0^\circ$  to  $180^\circ$ . Actually in our application it does not matter if the angle is  $0^\circ$  or  $180^\circ$ , as both indicate that the edge direction are in the horizontal direction. Therefore we will combine these two angles as follows,

$$\theta(x, y) = 0^\circ, \quad \text{if } \theta(x, y) = 180^\circ. \quad (7)$$

When both  $DF_x, DF_y$  are equal to zero, the pixel does not point to any direction but is an indication that the “activity” of the pixel is zero, or there is no intensity change around this pixel—these pixels are named “flat pixel.” For the convenience of calculation of the edge direction histogram, we assign a special angle,  $180^\circ$ , to it,

$$\theta(x, y) = 180^\circ, \quad \text{if } DF_x = 0 \text{ and } DF_y = 0. \quad (8)$$

Therefore the edge direction histogram is defined as,

$$\begin{aligned} \text{Histo}(k) &= \text{Histo}(k) + 1, \\ &\quad \text{if } \theta(x, y) = k, \text{ and } k \in [0, 180]. \end{aligned} \quad (9)$$

Figures 5 and 6 show the examples of edge direction histograms.

### 2.3 Measuring blocking artifacts using edge direction information

Typically, BDCT coding will result in discontinuity between neighboring blocks and also reduce the local activities of the image signal inside the blocks, thus reduce the image quality. This is more obvious when large quantization values are used during the coding process. Therefore we are able to define the blocking artifacts metrics based on the edge directional information after deriving the edge direction histogram as defined in Eq. 9.

As we have mentioned previously, the horizontal discontinuity between neighboring blocks will cause the edge pixel's orientation concentrating toward  $90^\circ$ , and vertical discontinuity between neighboring blocks will cause the edge pixel's orientation concentrating toward  $0^\circ$ . Therefore the percentage of the pixels with either  $0^\circ$  or  $90^\circ$  orientations indicates how severe the blocking artifacts are.

We define the horizontal and vertical discontinuity measures as,

$$B_{\text{IMAGE}} = \frac{\text{histo}(0) + \text{histo}(90)}{N_T \times \frac{24}{64}} = \frac{\text{histo}(0) + \text{histo}(90)}{0.375 \times N_T}, \quad (10)$$

where  $N_T$  is the total number of pixels in the image, and the coefficient 0.375 is a normalization factor that is determined by the percentage of pixels in the  $8 \times 8$  block (as in Fig. 3) marked with "H" and "V."

Note again that for  $\theta = 180$ ,  $\text{histo}(180)$  is an indication of the local activities of the image signal. Therefore, the signal activity measure of the image is defined as,

$$Z_{\text{IMAGE}} = \frac{\text{histo}(180)}{N_T \times \frac{36}{64}} = \frac{\text{histo}(180)}{0.5625 \times N_T}. \quad (11)$$

Similarly the coefficient 0.5625 is a normalization factor that is determined by the percentage of pixels in the  $8 \times 8$  block marked with "Z". It should be noted that in the calculation of histogram value  $\text{histo}[0]$ ,  $\text{histo}[1]$ , ...,  $\text{histo}[180]$ , we use all the pixels in an image. Although both  $B_{\text{IMAGE}}$  and  $Z_{\text{IMAGE}}$  give an indication of how severe the blocking artifacts are, their values are affected differently by the large quantization step size. As the bit rate in term of the bits per pixel drops at certain value,  $B_{\text{IMAGE}}$  starts dropping and  $Z_{\text{IMAGE}}$  starts increasing, indicating that the blocking artifacts become less severe due to the fact that many blocks merge and large uniform areas have been created, and the local activities have been reduced due to quantization values. On the other hand, for some pictures with large uniform areas such as clouds, sea, or walls, etc.,  $Z_{\text{IMAGE}}$  is very big even though the image is coded at very high bit rate. Based on the above analysis, we have chosen the following model to combine the above two individual measures to constitute a distortion assessment model,

$$DF_{\text{IMAGE}} = B_{\text{IMAGE}} + \beta \times B_{\text{IMAGE}} \times Z_{\text{IMAGE}}, \quad (12)$$

where the parameter  $\beta$  is determined experimentally to provide a better correlation with the subjective assessment of the distortion. In our experiments, we noticed that  $\beta = 1.64$  gives the best correlation with the subjective test data. It should be pointed out that  $DF_{\text{IMAGE}}$  is not very sensitive to the variation of  $\beta$  when it is within the range of 1–2.

It should also be noted that the above distortion metric is applicable to BDCT coded images without rotation. To apply  $DF_{\text{IMAGE}}$  to BDCT coded images with rotation such as the case in Fig. 6, we only need to change the angles used in Eq. 10 to be



the two maximum cells which are  $90^\circ$  apart. That is, we only need an extra step to find the maximum cells in the edge direction histogram before applying Eq. 10. Equations 11 and 12 keep unchanged in this case.

### 3 Experiments

In the following experiments, we used a number of still images, as well as frames from the test video sequences to test the performance of our algorithm. These images have different resolutions, ranging from  $176 \times 144$  to  $512 \times 512$ . Also, we use the  $3 \times 3$  uniform window to perform the gradient averaging. Examples of such images are Lena, Mandrill, Peppers, and video frames from Akiyo, Coastguard, Mobile, and Garden, etc. Fig. 7 shows the experimental results of applying  $DF_{\text{IMAGE}}$  to different images with different spatial complexity and resolution. It can be shown from these results that in general,  $DF_{\text{IMAGE}}$  achieves consistent results for all these images.

We have also tested our algorithm using the JPEG distortion database provided by Laboratory for Image and Video Engineering (LIVE) (Sheikh, Wang, Cormack, Bovik, 2002). LIVE Quality Assessment Database is designed by the LIVE at The University of Texas at Austin, with collaboration of the Department of Psychology at the University of Texas at Austin. In this database, 29 high-resolution 24-bits/pixel RGB color images (typically  $768 \times 512$ ) were compressed using JPEG with different compression ratios to yield a database of 204 images, 29 of which were the original (uncompressed) images. In order to get the subjective quality score of the images, each observer was shown the images randomly. Observers were asked to provide their perception of quality on a continuous linear scale that was divided into five equal regions marked with adjectives “Bad,” “Poor,” “Fair,” “Good,” and “Excellent.” The scale was then converted into 1–100 linearly. The testing was done in two sessions with about half of the images in each session.

The Pearson Correlation and Spearman rank-order Correlation between  $DF_{\text{IMAGE}}$  and the subjective ratings of the JPEG database are  $-0.9202$  and  $0.9036$ , respectively. After polynomial fitting, the fitted Pearson Correlation and Spearman rank-order

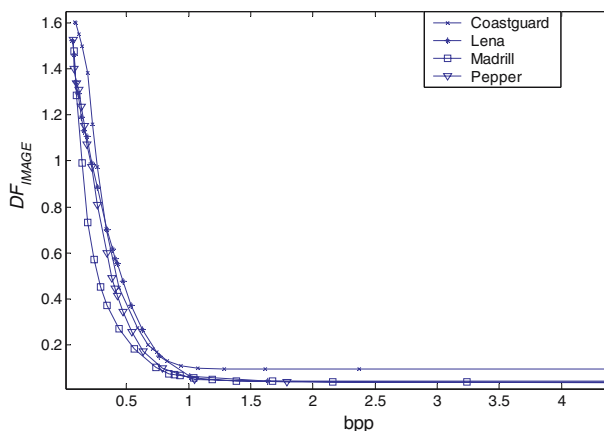
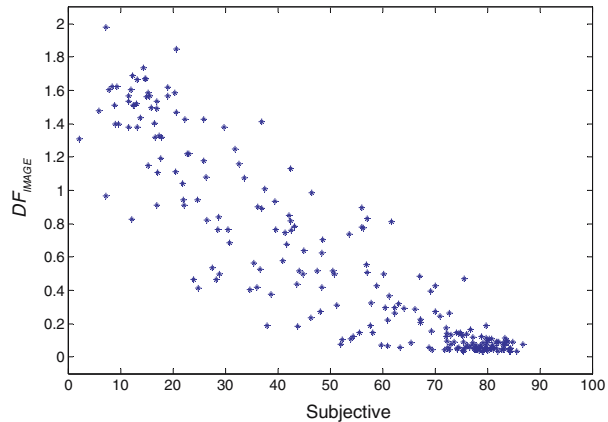


**Fig. 7**  $DF_{\text{IMAGE}}$  versus bits per pixel for different images

**Fig. 8** Scatter plot of applying  $DF_{\text{IMAGE}}$  to the images in LIVE database



Correlation between  $DF_{\text{IMAGE}}$  and the subjective ratings of the JPEG database are 0.9324 and 0.9042, respectively. This result shows that  $DF_{\text{IMAGE}}$  is very consistent with subjective ratings and thus is a very effective way of describing the subjective quality objectively. Figure 8 shows the scatter plot of applying  $DF_{\text{IMAGE}}$  to the images in LIVE database.

#### 4 Conclusions

This paper presents a novel un-referenced approach for measuring blocking artifacts in BDCT coding. Instead of using the traditional pixel discontinuity along the block boundary, we use the edge directional information of the images. Therefore the new algorithm does not need the exact location of the block boundary and is thus invariant to the displacement, rotation and scaling of the images. An additional advantage of the proposed measure is its well-defined value range and being very simple computationally.

Experiments show that the new distortion measure exhibits consistent results with various types of images and frame in video sequences. The new measure can be used as a distortion metric, a contributing factor in a quality metric, or a parameter controlling an encoding/post-processing process in real-time, in both referenced and un-referenced situations.

#### References

- Bazen, A. M., Gerez, S. H. (2002). Systematic methods for the computation of the directional fields and singular points of fingerprints. *IEEE Transactions on Pattern Analysis and Machine Intelligence*, 24, (7) 905–919.
- Gonzalez, R. C., Woods, R. E. (2002). *Digital image processing*. Englewood Cliffs, NJ: Prentice Hall.
- Karunasekera, S. A., Kingsbury, N. G. (1995) A distortion measure for blocking artifacts in images based on human visual sensitivity. *IEEE Transactions on Image Processing*, 4(6), 713–724.
- Kass, M., Witkin, A. (1987). Analyzing oriented patterns. *Computer Vision, Graphics, and Image Processing*, 37, 362–385.

- Miyahara, M., Kotani, K., Algazi, V. R. (1998). Objective picture quality scale (PQS) for image coding. *IEEE Transactions on Communications*, 46(9), 1215–1225.
- Sheikh, H. R., Wang, Z., Cormack, L., Bovik, A. C. (2002). *LIVE image quality assessment database*, <http://live.ece.utexas.edu/research/quality>.
- Shi, Y. Q., Sun, H. (1999). Image and video compression for multimedia engineering – fundamentals, algorithms and standards. Boca Raton: CRC Press.
- VQEG (2000). *Final report from the video quality experts group on the validation of objective models of video quality assessment*, <http://www.vqeg.org/>.
- Wang, Z., Sheikh, H. R., Bovik, A. C. (2002). No-reference perceptual quality assessment of JPEG compressed images. *2000 IEEE International Conference on Image Processing, Rochester, New York, September 22–25*, 1:477–480.
- Wu, H. R., Yuen, M. (1997) A generalized block-edge impairment metric for video coding. *IEEE Signal Processing Letters*, 4 (11) 317–320.
- Yu, Z., Wu, H. R., Winkler, S., Chen, T. (2002). Vision-model-based impairment metric to evaluate blocking artifacts in digital video. *Proceedings of the IEEE*, 90(1), 154–169.



**Feng Pan** (M'98–SM'01) received the B.Sc., M.Sc., and Ph.D. degrees in communication and electronic engineering from Zhejiang University, Hangzhou, China in 1983, 1986, and 1989, respectively. Since then, he has been teaching and researching in a number of universities in China, U.K., Ireland, and Singapore. His research areas are digital image processing, digital signal processing, digital video compression, and digital television broadcasting. He has published numerous technical papers and offered many short courses for industries. Dr. Pan was the Chapter Chairman of IEEE Consumer Electronics, Singapore from 2002 to 2004. He was also the general chairman of ISCE-2003, Sydney, Australia. He is currently serving as an associate editor of the International Journal of Innovational Computing & Information Control. Dr. Pan is now working as a video architect in ViXS Systems Inc., Toronto, Canada.

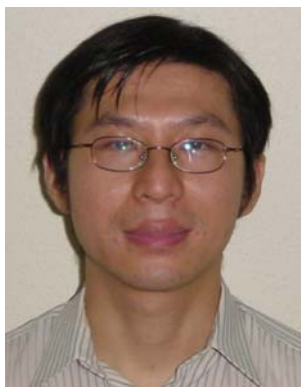


**Xiao Lin** received his Ph.D from Electronics and Computer Science Dept., University of Southampton, UK in 1993. He worked with Centre for Signal Processing (CSP) for about 5 years as a Research Fellow and Senior Research Fellow. After leaving CSP he joined DeSOC technology as a technical director. He then joined Institute for Infocomm Research in 2002, where he had been Member of Technical Staff, Lead Scientist and Principal Scientist and managed Media Processing Dept until 2006. He is now with Fortemedia Inc. He actively participated in the International Standards such as MPEG-4, JPEG2000, and JVT. He is a senior member of IEEE.



**Susanto Rahardja** received his Ph.D. in Electrical & Electronic Engineering from the Nanyang Technological University, Singapore. He joined the Centre for Signal Processing in 1996 and is a faculty member at the School of Electrical and Electronic Engineering in the Nanyang Technological University since 2001. In 2002, he joined the Institute for Infocomm Research (I2R). He is currently the director of Media Division in I2R where he oversees research areas on signal processing (audio coding, video/image processing), media analysis (text/speech, image, video), media security (biometrics, computer vision and surveillance) and sensor network. Dr. Rahardja has published more than 150 international journals and conferences in the area of digital communications, signal processing and logic synthesis. He was the recipient of the IEE Hartree Premium Award for best journal paper published in IEE Proceedings in 2001 and the Tan Kah Kee Young Inventors' Gold Award (Open Category) in 2003. He has served in various

IEEE and SPIE related professional activities in the area of multimedia and is actively involved in technical committee members of IEEE Circuits & Systems Society and Signal Processing Society. He is the Associate Editor of Journal of Visual Communication and Image Representation. Since 2002, he is an active participant of the MPEG and had since then involved in the development of MPEG-4 Audio where he is one of the main contributors to the MPEG-4 SLS and ALS. He received the Standards Council Merit Award 2006 from SPRING Singapore as recognition of significant contributions to the national standardization program.



**Ee Ping Ong** received the B.Eng. and Ph.D. degrees in electronics and electrical engineering from the University of Birmingham, Birmingham, U.K., in 1993 and 1997, respectively. From 1997 to 2001, he was with the Institute of Microelectronics, Singapore. Thereafter, he joined the Centre of Signal Processing, Nanyang Technological University, Singapore. Since 2002, he has been with the Institute for Infocomm Research, Singapore, where he is currently a Scientist. His research interests include motion estimation, video object segmentation and tracking, perceptual image/video quality metrics and coding.



**Weisi Lin** graduated from Zhongshan University, China with B.Sc and M.Sc in 1982 and 1985, respectively, and from King's College, London University, UK with Ph.D in 1992. He has worked in Zhongshan University, Shantou University (China), Bath University (UK), National University of Singapore, Institute of Microelectronics (Singapore), Centre for Signal Processing (Singapore), and Institute of Infocomm Research (Singapore). He has led over ten successful industrial-funded projects in digital multimedia since 1997, held eight patents and published over 90 refereed papers in international journals and conferences. His current research interests include image processing, perceptual visual distortion metrics, perceptual video compression and multimedia signal processing. Dr. Lin is a senior member of IEEE and a Chartered Engineer.